High Performance Computer Graphics, Multimedia and Visualisation
Volume 1, (2000), Number 1 pp. 1-20

A New Geometrical Support for the Radiosity Function†

Didier Arquès, Sylvain Michelin, Benoît Piranda

Équipe de synthèse d'images, Institut Gaspard Monge
Université de Marne la Vallée, 5 Boulevard Descartes, Champs sur Marne
F-77454 Marne la Vallée Cedex 2, France
e-mail: {arques,michelin,piranda}@univ-mlv.fr

Abstract

This paper focuses on a new radiosity approach. Using a new geometrical model that describes any surface with an atlas of "disk-like patches", i.e. a set of pieces covering the surface that can overlap each other, we express the radiosity function in a new function base. This leads to a new radiosity system where overlapping areas are taken into account. The classical radiosity approach appears now as a particular limit case of this new "overlapping radiosity".

Keywords: Complex surfaces, radiosity

1. INTRODUCTION

The main goal of rendering techniques is to simulate efficiently and precisely illumination phenomena. Researchers direct developments towards global models that simulate geometric optic [17], energetic behavior [7] or both, with for example two-pass algorithms [15] combining radiosity and ray-tracing. More recently, other complex phenomena like participating media [14], caustics [13] or diffraction or other wave optic phenomena [12] have also been studied.

In computer graphics, rendering techniques are directly linked to geometrical object representations. For instance, polygonal or parametric representations [5] are well-adapted to calculate the radiosity solution while implicit functions [2] or C.S.G. model [10] are more often used by ray-tracing algorithms [6]. The goal of any radiosity approach is to solve the rendering equation [11]. In general, finite element analysis is used: the radiosity solution is expressed in set (a base) of functions which are linked to a geometrical support. We can classify radiosity approaches in two categories:

– first classical solutions [7] consist in meshing surfaces in a set of patches on which the energy (radiosity) is supposed to be constant. The energetic balance of each patch leads to the classical form factor expression and to the resolution of a linear system [4]. After resolution, the radiosity function is reconstructed for example by a Gouraud's shading. Considering the finite element point of view, we just approximate the radiosity function in a set of constant functions ("box" function) defined locally for each patch. The main advantage of these methods is the simplicity of the functions (a unique constant function for each patch) and of the support (local to the patch). A lot of terms maintain geometrical meaning: for example the form factor still has a physical meaning and classical developments (Stokes's theorem. . .) can be efficiently used. Moreover, complex variations of the radiosity function can be treated only by subdividing the geometrical support. In the other hand, these methods imply complex data structures to maintain the surface topology, especially if hierarchical representations [9] or automatic adaptive meshing algorithms [3] are used.

– in recent works, other function bases, easily integrable are used. H.R. Zatz in [18] proposes to express the radiosity function in a set of polynomial functions (Legendre polynomials), while Gorthler et al. apply wavelet analysis [8]. A parametric definition of the surfaces is used to support each function of the base. Under these assumptions we loose advantages of the local support, because we work in a parametric space. Moreover, complex variations of the radiosity function impose unfortunately to increase the number of functions in the base.

Here, we propose a new complete model which avoids efficiently some of these previous drawbacks. The first part of this paper (section 2) presents this new radiosity approach while section 3 presents implementation aspects. Results are discussed in section 4.

† First presented at WSCG'2000

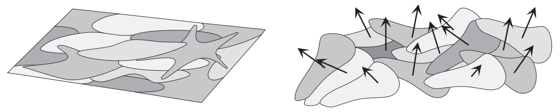

(a) (b)

Figure 1: *Disk-like patches on a planar surface (a) and a non plane surface (b).*

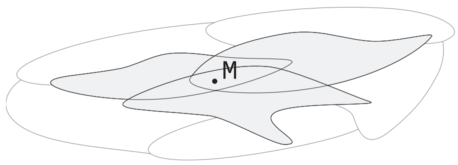

Figure 2: *Only gray disk-like patches cover the point M.*

2. A NEW RADIOSITY APPROACH

2.1. A New Base of Functions with Local Support

In a previous paper [1], we propose a new approach for the modeling and the rendering of complex surfaces. In this model, any surface S is defined by *a covering atlas of disk-like patches*, i.e. a set of N_S disk-like patches $\{D_i, i = 1 \dots N_S\}$ verifying the following properties. Disk-like patches:

- are open surfaces (not necessary planar);
- approximate locally as close as possible the surface;
- can overlap each other contrary to classical polygonal patches;
- cover entirely the surface.

Figure 1 shows two examples of surfaces represented by an atlas of disk-like patches.

As discussed in section 4.1 this model is an interesting alternative to polygonal meshes because it simplifies the geometry complexity by decreasing topological constraints. Problems of complex geometrical construction and storage disappear.

In this section we propose to use the atlas of disks as the local geometrical support of a new set of function bases. Then, for each point M of the surface the luminance $L(M)$ is decomposed in a base of functions associated to the set of N disks covering M (see figure 2) according to:

$$L(M) = \sum_{i=1}^{N} L_i(M)\alpha_i(M) \qquad (1)$$

where the two following functions α_i and L_i are associated to a disk D_i:

- $\alpha_i(M)$ can be seen as the probability of the presence at M of the disk-like patch D_i among the N_S disks of the atlas.
- $L_i(M)$ are the coefficients associated to each function.

The definition of the α functions implies that:

$$\begin{cases} \alpha_i(M) > 0 & if\ M \in D_i \\ \alpha_i(M) = 0 & if\ M \notin D_i \end{cases}$$

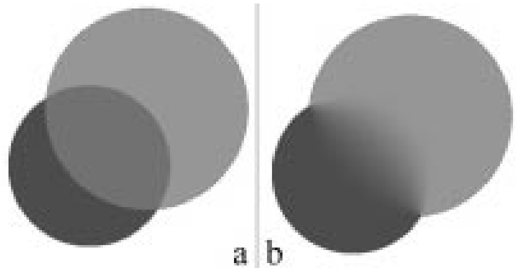

Figure 3: *A simple example of reconstruction of $L(M)$.*

and that

$$\sum_{i=1}^{N} \alpha_i(M) = 1$$

In order to simplify the choice of the presence functions $\alpha_i(M)$, we associate to each patch D_i a function $\beta_i(M)$ that verifies:

$$\begin{cases} \beta_i(M) > 0 & if\ M \in D_i \\ \beta_i(M) = 0 & if\ M \notin D_i \end{cases}$$

and we define:

$$\alpha_i(M) = \frac{\beta_i(M)}{\sum_{j=1}^{N} \beta_j(M)}$$

Considering that $\alpha_i(M)$ is null outside the disk D_i, equation (1) can also be written in:

$$L(M) = \sum_{i/M \in D_i} L_i(M)\alpha_i(M) \qquad (2)$$

This approach allows us to take into account advantages of the two previous solution categories:

– As a unique function $\beta_i(M)$ is associated to each disk-like patch (its local support), no parametric surface representation is needed. Moreover the geometrical atlas model allows us to express in the same way a very large variety of surfaces.

– In a superposition area, i.e. in a point M covered by a set of disk-like patches, a variable number of functions is used to expressed the value in $F(M)$. This number depends here on the geometrical disposition of the disk-like patches on the surface, while it is fixed in a Galerkin approach.

Figure 3 represents two disks in the same plane and admitting an overlapping area. We suppose that the luminance (or color) of each disk is known: constant, red for the first one and green for the second one. We apply equation (2) to reconstruct the luminance function over the two disks. In figure 3a we choose a very basic function β_i constant and equal to 1 for each point of the disk and equal to 0 outside the disk. Then, the application of equation (2) imply that the common area of the two disks is filled by a uniform average luminance (or color). If β_i is a function which varies continuously from 1 in the center of the disk to 0 in the border, it is easy to verify that $L(M)$ varies continuously too from one color to the other in the overlapping area (figure 3b).

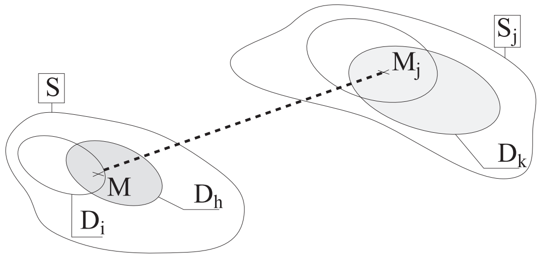

Figure 4: *Geometry of the energy exchanged between disk-like patches.*

2.2. Developing the Radiosity Solution

In this section, we consider that each surface describing a scene is represented by an atlas of disk-like patches and we present a complete radiosity approach which takes into account this hypothesis. The method we propose here is similar to the classical radiosity approach: an energy balance allows us to compute a radiosity value (supposed constant) for each disk.

Even if we develop the radiosity solution in a set of basis functions, this approach differs from the Galerkin method for many reasons. In the classical Galerkin approach, H.R. Zatz uses a set of orthogonal functions that allows to simplify the calculus of the coefficients by a classical inner product. In our approach, the function basis is not necessarily orthogonal. Moreover no dual basis can be directly obtained because the function α is too complex, depending on the overlapping areas between neighboring disks. As a consequence, classical developments of the Galerkin method can not be applied and a solution consists in substituting equation 1 in both left and right sides of the rendering equation.

2.2.1. Rewriting the Rendering Equation

If we consider a point M of a given surface S (cf. figure 4), the energy living this point is classically expressed by the following energy balance equation [16] expressed in term of radiosity:

$$B(M) = E(M) + \rho(M)H(M) \quad (3)$$

where $E(M)$ is the self radiosity (exitance), $\rho(M)$ the diffuse reflectance and $H(M)$ the illumination of M:

$$H(M) = \sum_j \int_{S_j} B(M_j)F(M,M_j)dM_j$$

where M_j is a point of the surface S_j and $F(M,M_j)$ is the classical elementary form factor between the two elementary surfaces centered on M and M_j. It includes the visibility term, i.e. $F(M,M_j) = 0$ if there is another object between M and M_j. Following the previous developments (section 2.1), equation (2) is used to express the radiosity, the reflectance coefficient and the exitance of M. We have:

$$\begin{aligned} B(M) &= \sum_{i/M\in D_i} \alpha_i(M)B_i(M) \\ E(M) &= \sum_{i/M\in D_i} \alpha_i(M)E_i(M) \\ \rho(M) &= \sum_{i/M\in D_i} \alpha_i(M)\rho_i(M) \end{aligned}$$

where the index i identifies the disk-like patches D_i of S that cover M (cf. figure 4).

Substituting these relations in equation (3) gives:

$$\begin{aligned} \sum_{i/M\in D_i} \alpha_i(M)B_i(M) = &\sum_{i/M\in D_i} \alpha_i(M)E_i(M) \\ &+H(M)\sum_{i/M\in D_i} \alpha_i(M)\rho_i(M) \end{aligned} \quad (4)$$

To simplify the development, the different terms of this equation are treated separately.

2.2.2. Development of $H(M)$

First, we consider $H(M)$ and we substitute $B(M_j)$ by its expression. We obtain:

$$H(M) = \sum_j \int_{S_j} \sum_{k/M_j\in D_k} \alpha_k(M_j)B_k(M_j)F(M,M_j)dM_j$$

where k identifies disk-like patches covering the point M_j. The presence function $\alpha_k(M_j)$ being null outside the disk D_k, we can write:

$$H(M) = \sum_j \sum_{k/D_k of S_j} \int_{D_k} \alpha_k(M_j)B_k(M_j)F(M,M_j)dM_j$$

Finally, if N_D is the total disk number of the scene, we can rewrite this expression by simplifying the double sum:

$$H(M) = \sum_{k=1}^{N_D} \int_{D_k} \alpha_k(N)B_k(N)F(M,N)dN \quad (5)$$

where N_D represents any point of any surface S_j and where k now identifies each disk-like patch of the scene.

2.2.3. A New Radiosity Equation

The last step consists in integrating equation (4) over the disk-like patch D_h of S (see figure 4), in order to obtain the radiosity of each disk-like patch.

$$\begin{aligned} &\int_{D_h} \sum_{i/M\in D_i} \alpha_i(M)B_i(M)dM = \\ &\int_{D_h} \sum_{i/M\in D_i} \alpha_i(M)E_i(M)dM \\ + &\int_{D_h} \sum_{i/M\in D_i} \alpha_i(M)\rho_i(M)H(M)dM \end{aligned} \quad (6)$$

We first develop:

$$I_1 = \int_{D_h} \sum_{i/M\in D_i} \alpha_i(M)B_i(M)dM \quad (7)$$

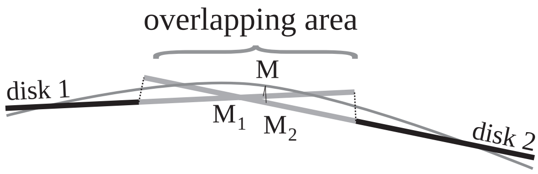

Figure 5: *Example of association of points M_i that approximate M for each disk D_i.*

Considering homogeneous overlapped areas of the disk D_h, equation (7) becomes:

$$I_1 = \sum_{i/D_i \cap D_h \neq \emptyset} \int_{D_h} \alpha_i(M) B_i(M) dM \qquad (8)$$

This expression is exact for planar surfaces, but has to be approximated in the case of non planar surfaces. In a superposition area (cf. figure 5) each point M of S is associated to the points M_i of the disks D_i which overlap M. Simple algorithms [1] are used. Equation 8 becomes:

$$I_1 \approx \sum_{i/D_i \cap D_h \neq \emptyset} \int_{D_h} \alpha_i(M_i) B_i(M_i) dM$$

In this case $D_i \cap D_h$ corresponds to the overlapping area between D_i and D_h.

We now develop:

$$I_2 = \int_{D_h} \sum_{i/M \in D_i} \alpha_i(M) \rho_i(M) H(M) dM$$

By substituting $\rho(M)$ by a similar expression of equation (8) and $H(M)$ by (5), we obtain:

$$\begin{aligned} I_2 = & \sum_{i/D_i \cap D_h \neq \emptyset} \int_{D_h} \rho_i(M) \alpha_i(M) \times \\ & \sum_{k=1}^{N_D} \int_{D_k} \alpha_k(N) B_k(N) F(M,N) dN dM \end{aligned}$$

If, as in a classical radiosity approach, we suppose that the radiosity, the exitance and the reflectance are constant over each disk, ($B_i(M) = B_i$, $E_i(M) = E_i$ and $\rho_i(M) = \rho_i$), equation (6) becomes:

$$\begin{aligned} & \sum_{i/D_i \cap D_h \neq \emptyset} B_i \int_{D_h} \alpha_i(M) dM = \\ & \sum_{i/D_i \cap D_h \neq \emptyset} E_i \int_{D_h} \alpha_i(M) dM + \sum_{i/D_i \cap D_h \neq \emptyset} \rho_i \times \\ & \sum_{k=1}^{N_D} B_k \int_{D_h} \int_{D_k} \alpha_i(M) \alpha_k(N) F(M,N) dN dM \end{aligned}$$

If we define: $c_{ih} = \int_{D_h} \alpha_i(M) dM$ and

$$F_{ih|k} = \int_{D_h} \int_{D_k} \alpha_i(M) \alpha_k(N) F(M,N) dN dM$$

a new form factor defined between the portion $D_i \cap D_h$ and another disk D_k, we finally obtain for each disk-like patch D_h:

$$\begin{aligned} & \sum_{i/D_i \cap D_h \neq \emptyset} B_i c_{ih} = \sum_{i/D_i \cap D_h \neq \emptyset} E_i c_{ih} \\ & + \sum_{i/D_i \cap D_h \neq \emptyset} \rho_i \sum_{k=1}^{N_D} B_k F_{ih|k} \end{aligned} \qquad (9)$$

2.3. Matrix Representation

The expression of equation (9) for each disk-like patch D_h leads to a linear system of equations. We express it using a matrix form. Because c_{ih} is null if $D_i \cap D_h = \emptyset$ for any disk-like patch D_h, we obtain:

$$\sum_{i=1}^{N_D} \left(c_{ih} - \sum_{j/D_j \cap D_h \neq \emptyset} \rho_j F_{jh|i} \right) B_i = \sum_{i=1}^{N_D} c_{ih} E_i$$

or finally in matrix form $M \times B = C \times E$ with

$$M_{ih} = c_{ih} - \sum_{j/D_j \cap D_h \neq \emptyset} \rho_j F_{jh|i}$$

2.4. Classical Radiosity Retrieval

It is interesting to see that this new energy balance (9) is a generalization of the classical radiosity. Equation (9) can be simplified to retrieve classical radiosity equation in the case of a classical mesh. If overlapping areas tend towards zero, only D_h has a superposing area with itself. So, equation (9) becomes:

$$B_h c_{hh} = E_h c_{hh} + \rho_h \sum_{k=1}^{N_D} B_k F_{hh|k}$$

In the same time, the presence function $\alpha_i(M)$ is constant, equal to 1 for each point M of D_h, so:

$$c_{hh} = \int_{D_h} \alpha_h(M) dM = A_h$$

where A_h is the surface of the disk-like patch D_h.

For the same reason, the new form factor expression $F_{hh|k}$ is simplified in:

$$\begin{aligned} F_{hh|k} &= \int_{D_h} \int_{D_k} V \frac{\cos\theta_h \cos\theta_k}{\pi r^2} dM dN \\ &= A_h F_{hk} \end{aligned}$$

where F_{hk} is the classical form factor, and V the occlusion function.

We finally retrieve the classical radiosity equation:

$$A_h B_h = A_h E_h + A_h \rho_h \sum_{k=1}^{N_D} B_k F_{hk}$$

3. IMPLEMENTATION

In this section, we describe an implementation of the overlapping radiosity method. As in classical radiosity, we use a two-pass algorithm. The first pass consists in resolving the radiosity system (9), and the second pass uses a view-dependent algorithm that computes the final image. An approach similar to the progressive refinement algorithm [4] can be developed for the first pass. We express the contribution of the unshot radiosity of D_k to the radiosity and the unshot radiosity of any other disk D_h. But contrary to classical radiosity, this energy has to be distributed to the disks that overlap D_h (including D_h). The energy contribution (in Watt) of the unshot radiosity ΔB_k of the disk D_k to the radiosity of the disks overlapping D_h is defined by:

$$EC = \sum_{i/D_i \cap D_h \neq \emptyset} \rho_i F_{ih|k} \Delta B_k$$

This energy must be distributed to the disks overlapping D_h in order to verify:

$$\sum_{i/D_i \cap D_h \neq \emptyset} \Delta B_i c_{ih} = EC$$

It can trivially be realized by adding the following proportion

$$\frac{c_{ih}}{\sum_{j/D_j \cap D_h \neq \emptyset} c_{jh}} EC$$

to each disk D_i. Using $\sum_{j/D_j \cap D_h \neq \emptyset} c_{jh} = A_h$ the surface of the disk D_h, this energy variation corresponds to the following radiosity variation:

$$\Delta B_i = \frac{c_{ih}}{A_h} \frac{EC}{A_i}$$

This development leads to the following algorithm: // initialization for each disk Dh do DeltaBh = Eh Bh = Eh end do // shooting process repeat // select the emitter Dk Dk = disk of maximum Ckk*DeltaBk // computing the total energy received by Dh Ec = 0 for each disk Di overlapping Dh do compute Fihk Ec += Fihk*Rhoi*DeltaBk end do // dispatching energy for each disk Di overlapping Dh do Drad = Ec*Cih/(Ah*Ai) Bi += Drad DeltaBi += Drad end do end do // put unshot radiosity of Dk to 0 DeltaBk = 0 until convergence

4. RESULTS AND DISCUSSION

4.1. Modeling Considerations

In image 6, we show the geometrical disposition of the disk-like patches.

This scene shows a room containing a cubic box, lighted by a spotlight. We use here two kinds of disk-like patches: disks and squares. Squares allow us to define precisely the edges of the box, but other modeling approaches may be used (smaller disks on borders for instance). Modeling objects with an atlas of disk-like patches gives us a large choice of disk shapes and positions. For example, the previous regular disposition of the disks is not necessarily the best choice and any random disposition does not change the complexity of the treatments.

This new surface model efficiently simplifies the geometry complexity by decreasing topological constraints between disk-like patches. Problems of complex geometrical construction and storage disappear.

Any object is described by just a simple list of disk-like patches. As a consequence, simple or complex surfaces are similarly defined, and efficiently treated by this method as shown in figure 8 (a sand heap), figure 9 (a cave wall) and

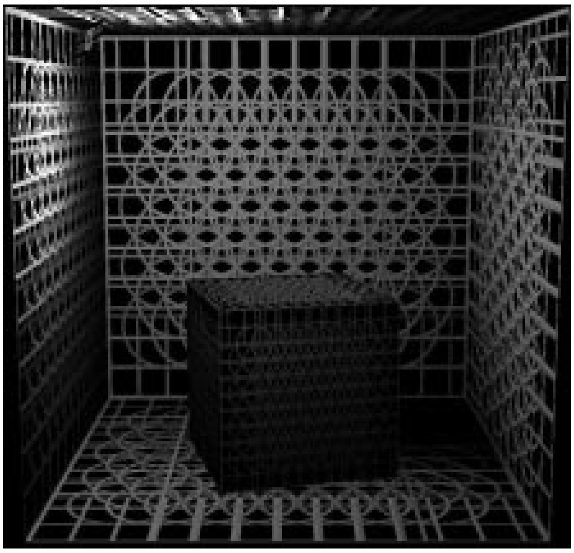

Figure 6: *Geometry of the disk-like patches.*

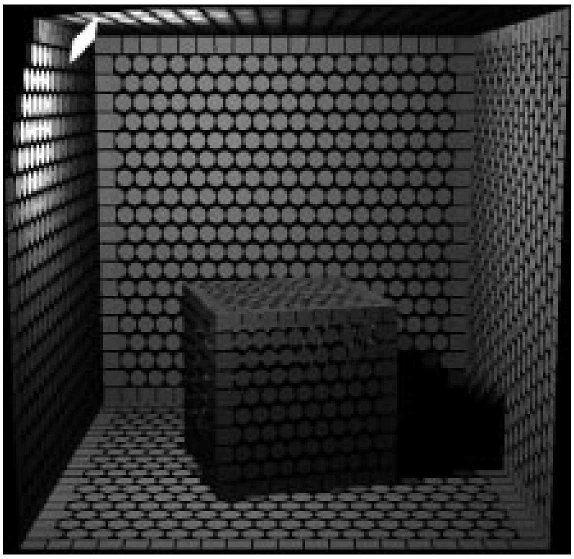

Figure 7: *Small disks without any overlapping area.*

figure 10 (a tunnel). It also explains that some of our actual works concern adaptive subdivision algorithms that are plenty simplified because we do not have to store and update a complex geometry representation.

4.2. Rendering Considerations

It is also interesting to point out that the different levels of rendering are obtained by the same algorithm with different β functions. Figure 11 shows the previous scene rendered with a function constant for any disk-like patch. This choice underlines overlapping areas between disk-like patches. In the last image 12, we use a β function that is varying continuously from 1 in the center of the disk to 0 in the border of each disk to obtain a more realistic rendering.

Figure 8: *a sand heap.*

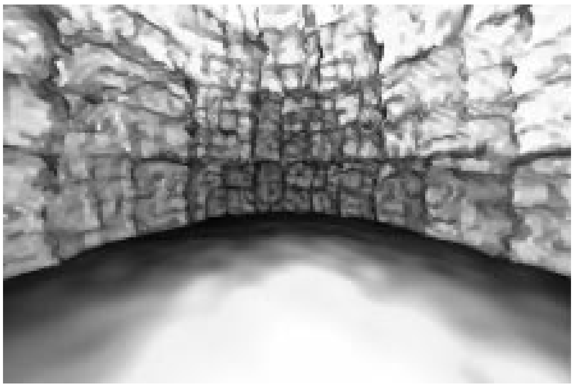

Figure 9: *a cave.*

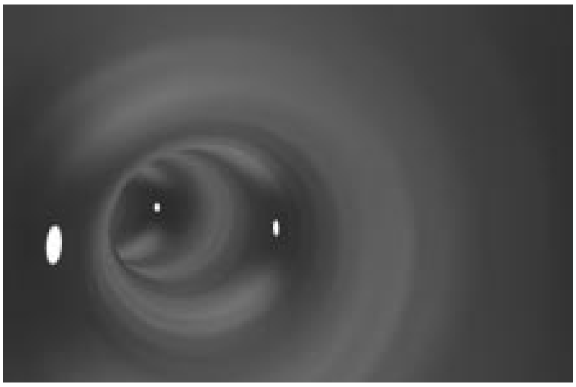

Figure 10: *the interior of a tunnel.*

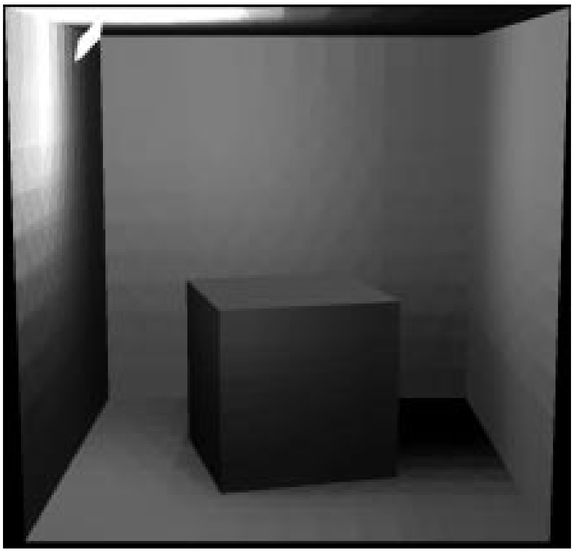

Figure 11: *Case of a function* β_i *constant.*

In the classical radiosity approach, different artifacts are due to the polygonal mesh and to the preponderant directions used in Gouraud shading. These artifacts disappear with our method because circular disks admit no preponderant directions and because overlapping areas blur efficiently the limits of the disks.

Computational times are similar to those obtained with a classical radiosity approach but. In a first step, the overlapping areas are computed and stored with the geometrical database then the complexity of a step in the progressive refinement algorithm is obviously $O(N_D)$ where the complexity of the same step in the classical radiosity algorithm is $O(patchnumber)$. For example, considering the scene of figure 10 that is described by about 6400 disks, computational time due to one iteration of the progressive refinement algorithm is about 15 seconds (on a Pentium II 450 personal computer).

5. CONCLUSION

In this paper we present a new radiosity approach for the rendering of a large variety of surfaces. We use a new geometrical model that consists in a set of disk-like patches that can overlap each other. This geometrical model allows us to propose a new interesting base of local functions for solving the rendering equation. As a consequence, classical rendering artefacts due to polygonal mesh desappears and the use of the β function leads to a large set of possibilities both for modeling and rendering aspects. The resulting "overlapping radiosity" generalizes previous radiosity approaches to overlapping patches.

References

1. D. Arques, S. Michelin, and B. Piranda. Implicit Surfaces Driven by an Atlas of Discoids. In *Graphicon'00*, pages 256–261, 2000.

2. J. Blinn. A generalization of algebraic surface drawing.

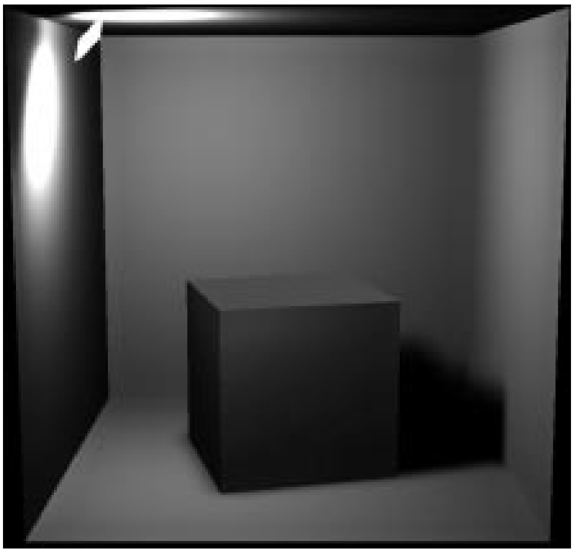

Figure 12: *Case of a function β_i that varying continuously from 1 to 0.*

In *ACM Transactions on Graphics*, volume 1(3), pages 235–256, 1982.

3. A. T. Campbell and D. S. Fussell. Adaptive Mesh Generation for Global Diffuse Illumination. In *Computer Graphics (ACM SIGGRAPH '90 Proceedings)*, volume 24(4), pages 155–164, Aug. 1990.

4. M. Cohen, S. Chen, J. Wallace, and D. Greenberg. A Progressive Refinement Approach for Fast Radiosity Image Generation. In *Siggraph'88, Computer Graphics*, volume 22(4), pages 74–84, 1988.

5. J. Foley, A. V. Dam, S. Feiner, and J. Hugues. *Computer graphics: principles and practice*. Addison Wesley, 2nd edition, 1990.

6. A. Glassner. *An Introduction to ray-tracing*. Academic Press, 1989.

7. C. Goral, K. Torrance, D. Greenberg, and B. Battaile. Modeling the interaction of light between diffuse surfaces. In *Siggraph'84, Computer Graphics*, volume 18(3), pages 213–222, 1984.

8. S. J. Gortler, P. Schroder, M. F. Cohen, and P. Hanrahan. Wavelet Radiosity. In *Computer Graphics Proceedings, Annual Conference Series, 1993 (ACM SIGGRAPH '93 Proceedings)*, pages 221–230, 1993.

9. P. Hanrahan, D. Salzman, and L. Aupperle. A Rapid Hierarchical Radiosity Algorithm. In *Computer Graphics (ACM SIGGRAPH '91 Proceedings)*, volume 25(4), pages 197–206, July 1991.

10. F. W. Jansen. A CSG list priority hidden surface algorithm. In *Proceedings of the Eurographics'85*, pages 51–62, 1985.

11. T. Kajiya. The Rendering Equation. In *Computer Graphics (ACM SIGGRAPH '86 Proceedings)*, volume 20(4), pages 143–150, Aug. 1986.

12. M. Lucente and T. Galyean. Rendering interactive holographic images. In *Siggraph'95, Computer Graphics, annual conference series*, pages 387–394, 1995.

13. T. Nishita and E. Nakamae. Method of displaying optical effects within water using accumulation buffer. In *Siggraph'94, Computer Graphics, annual conference series*, pages 373–379, 1994.

14. H. Rushmeier and K. Torrance. The zonal method for calculating light intensities in the presence of participating medium. In *Siggraph'87, Computer Graphics*, volume 21(4), pages 293–302, 1987.

15. F.-X. Sillion and C. Puech. A general two-pass method integrating specular and diffuse reflection. In *Siggraph'89, Computer Graphics*, volume 23(3), pages 335–344, 1989.

16. F.-X. Sillion and C. Puech. Radiosity and global illumination. In *Morgan Kaufmann Publishers Inc.*, 1994.

17. T. Whitted. An improved illumination model for shaded display. In *Communication of the ACM*, volume 23(6), pages 343–349, 1980.

18. H. R. Zatz. Galerkin Radiosity: A Higher Order Solution Method for Global Illumination. In *Computer Graphics Proceedings, Annual Conference Series, 1993 (ACM SIGGRAPH '93 Proceedings)*, pages 213–220, 1993.